HHS Public Access

Author manuscript

J Am Chem Soc. Author manuscript; available in PMC 2019 December 05.

Published in final edited form as:

J Am Chem Soc. 2018 December 05; 140(48): 16433–16437. doi:10.1021/jacs.8b10542.

Instructed-Assembly of Peptides for Intracellular Enzyme Sequestration

Zhaoqianqi Feng, **Huaimin Wang**, and **Bing Xu**[*]

Department of Chemistry, Brandeis University, 415 South Street, Waltham, Massachusetts 02454, United States.

Abstract

Liquid-like droplets of biomacromolecules are emerging as a fundamental mechanism of cellular signaling, but designing synthetic mimics to form such membraneless organelles remains unexplored. Here we report the use of supramolecular assemblies of small peptides, as a mimic of biomacromolecular condensates, for intracellular sequestration of enzymes on endoplasmic reticulum (ER). Specifically, integrating a short peptide with naproxen (a nonsteroidal anti-inflammatory drug (NSAID) and a ligand of cyclooxygenase-2 (COX-2)) generates an enzymatic substrate that acts as a precursor for instructed-assembly. Slowly dephosphorylating the precursors by phosphatases forms the corresponding hydrogelators in cellular environment, which results in the supramolecular assemblies on ER. Consisting of the precursor and the hydrogelator molecules, the assemblies enable the sequestration of COX-2 and protein-tyrosine phosphatase 1B (PTP1B) on ER. Further structure-activity investigation reveals that the co-localization of COX-2 and PTP1B relies on the NSAID motif, the phosphotyrosine, and the enzymatic dephosphorylation of the precursor. This work, for the first time, illustrates the use of supramolecular processes for associating enzymes in cells, and may provide insights for understanding intracellular liquid condensates and a new strategy for modulating protein-protein interactions.

Graphical Abstract:

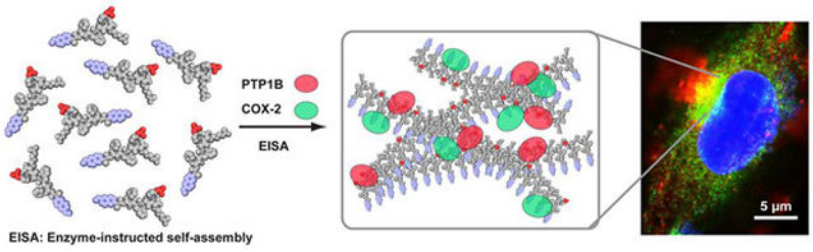

[*]**Corresponding Author** bxu@brandeis.edu.

Supporting Information

Materials, detailed experimental procedures, additional figures. This material is available free of charge via the Internet at http://pubs.acs.org.

Notes

The authors declare no competing financial interest.

It is known that biomacromolecules are able to form liquid-phase condensates, such as Cajal bodies,[1] U and P bodies,[2] and nucleolus,[3] inside cells via liquid-liquid phase separation. Recent studies have suggested that such a liquid phase condensation likely represents a ubiquitous cellular process for organizing intracellular space and for cellular signalings.[4] For example, the binding of DNA to cyclic GMP–AMP synthase (cGAS) results in liquid droplets that concentrate an enzyme and reactants to activate innate immune signaling.[5] Despite these exciting developments[6,7] in biology, the use of synthetic molecules to mimic these membraneless organelles has yet to be explored. The key feature of liquid phase condensates is the non-covalent association of molecules at a high concentration to result in a liquid-liquid phase transition. This process coincides with sol-to-gel transition, a type of liquid-liquid phase transition, which is a usual consequence of enzyme-instructed self-assembly (EISA).[8,9] Thus, we decide to use EISA to generate supramolecular assemblies of peptides in cellular environment to mimic the membraneless organelles for enzyme sequestration.

As a form of instructed-assembly,[10] EISA refers to the formation of ordered superstructures of molecules as the consequence of enzymatic reactions. Like self-assembly, EISA relies on non-covalent interactions to form the assemblies from small, simple building blocks; unlike self-assembly, EISA includes an enzymatic reaction, a process that is away from equilibrium ($\Delta G < 0$) and inherently irreversible.[10] Recent studies have already demonstrated the promising applications of supramolecular assemblies in biomedicine,[11–14] particularly the use of EISA of small molecules for selectively inhibiting cancer cells in vitro,[15–19] for slowing tumor progression in animal models,[20–23] and for molecular imaging applications.[24–26] These promising developments imply that EISA generated supramolecular assemblies of small molecules should be able to mimic the biomacromolecular condensates (e.g., membraneless organelles) in cellular environment.

To demonstrate the concept of EISA for sequestration of enzymes, we use EISA to generate supramolecular assemblies to interact with multiple numbers of cyclooxygenase-2 (COX-2) and protein-tyrosine phosphatase 1B (PTP1B) simultaneously. Based on above concept, we designed EISA precursor **Npx-1P**, which consisted of a NSAID drug (naproxen), a self-assembling D-peptide backbone (D-Phe-D-Phe), an enzyme trigger (D-phosphotyrosine), and a positively charged homoarginine residue at the C-terminal. Such a design allows **Npx-1P** to interact selectively with COX-2[27] and to serve as a substrate for PTP1B[28] simultaneously. Moreover, the use of homoarginine allows the supramolecular assemblies to form on ER via EISA as evidenced by our previous report that the fluorescent analogue of **Npx-1P** forms enzymatic assemblies on ER of cancer cells.[29] As illustrated in Scheme 1, partially dephosphorylated by phosphatases, the precursor (**Npx-1P**) and its corresponding hydrogelator (**Npx-1**) co-assemble to form supramolecular assemblies that promote the association of COX-2 and PTP1B on endoplasmic reticulum (ER). Critical micelle concentration (CMC) measurement and transmission electron microscopy (TEM) confirm that enzymatic conversion of **Npx-1P** to **Npx-1** results in increased self-assembling propensity and the phase transition (sol-gel). The formed supramolecular assemblies enrich COX-2 and PTP1B in a cell free condition, as evidenced by the TEM images and pull down analysis. Immunofluorescence staining indicates that the nanofibers, forming in cellular

environment, interact with COX-2 and PTP1B and induce their association at ER of cells (Saos-2[30]). Structure-activity relationship studies reveal that the COX-2 binding NSAID motif and the phosphatase substrate are essential for the association of the enzymes. As the first demonstration of EISA as a molecular process to enable intracellular sequestration of enzymes, this work illustrates enzymatic non-covalent synthesis of molecular condensates in cellular environment for conferring biological functions to supramolecular assemblies, a future direction of supramolecular chemistry.[31]

After synthesizing the precursor **Npx-1P** via solid-phase peptide synthesis,[32] we first examined its liquid-liquid phase transition. Upon the addition of alkaline phosphatase (ALP), the **Npx-1P** undergoes a sol–gel transition when the concentration is about 400 μM (Figure 1A, Figure S9) in PBS buffer. We used liquid chromatography–mass spectrometry (LC-MS) and TEM to examine the enzymatic dephosphrylation of **Npx-1P** and the generation of supramolecular assemblies. **Npx-1P** hardly forms any ordered nanostructure at the concentration of 12.5 μM (Figure S10), agreeing with the CMC of **Npx-1P (**35 μM**)** **(**Figure 1B) in PBS buffer. The addition of ALP to the solution of **Npx-1P** in PBS for half an hour dephosphorylates 15% of **Npx-1P** to **Npx-1** (Figure 1C) to form aggregates (Figure 1D). After 1 h incubation, the amount of dephosphorylated **Npx-1P** increases to 29%, which yields an **Npx-1** concentration of 3.6 μM. While the concentration of **Npx-1** in the above solution (3.6 μM) is lower than the CMC of **Npx-1** (5.7 μM), short nanofibers form with a width of 7 ± 2 nm, suggesting the participation of **Npx-1P** at the mixture in the assembly process. The structural similarity between **Npx-1P** and **Npx-1** favors their co-assemblies, as evidenced by the nanofibers with a uniform width of 7 nm in Figure 1D, since **Npx-1P** itself only forms uniform nanofibers with a width of 5 nm. (Figure S11) These results are similar to the previous reports of peptide coassembly.[33,34] From 1 h to 2 h, the short nanofibers grow to long uniform nanofibers as 50% of **Npx-1P** being converted into **Npx-1**. Moreover, the dephosphorylation rate of **Npx-1P** by ALP decreased after 2 h incubation, (Figure S12) likely due to the co-assembly of **Npx-1P** and **Npx-1**, which reduces the amount of free **Npx-1P**. These results verify the phase/morphological transition resulted from EISA of **Npx-1P** and indicate the co-assembly of **Npx-1P** and **Npx-1**.

We then investigated the interactions between enzymatically formed assemblies and the enzymes (COX-2 and PTP1B). Being co-incubated with **Npx-1P** and after the addition of ALP, either PTP1B or COX-2 adheres to the nanofibers of **Npx-1P** and **Npx-1** (Figure S13). The incubation of COX-2 and PTP1B with **Npx-1P** and ALP results in larger protein aggregates on the nanofibers. Some of the proteins appear to be away from the nanofibers in the TEM image, which are likely due to the dynamic nature of enzymatic assemblies. These observations suggest interaction and enrichment of COX-2 and PTP1B on the non-covalent assemblies formed by enzymatically dephosphorylation of **Npx-1P**. To further confirm the interactions between assemblies and proteins, we conducted the pull-down assay of PTP1B and COX-2 with the enzymatic assemblies (Figure 2), which reveals that the pellet, compared with the supernatant, of assemblies abundantly enrich both PTP1B and COX-2, further validating the enzyme sequestration by the supramolecular assemblies formed by EISA. In addition, after 1 h incubation, PTP1B (45 U/mL) converted 50%, 40% and 25% of **Npx-1P** to **Npx-1** when the concentration of **Npx-1P** is 50 μM, 100 μM and 200 μM,

respectively, but hardly hydrolyzed more **Npx-1P** from 1 h to 24 h (Figure S14). This observation likely results from the sequestration of PTP1B from solution to the assemblies, which reduces the amount of free enzymes.

To verify the enzymatic transformation and self-assembly of **Npx-1P** in live cells, we quantified the conversion of **Npx-1P** after incubating it with Saos-2 cells at different time points. Figure 3A indicates that endogenous phosphatases convert 19%, 29%, and 46% of **Npx-1P** to **Npx-1** after 0.5 h, 1 h, and 2 h incubation, respectively. This result implies the co-assembly of **Npx-1P** and **Npx-1** in live cells, agreeing with the results from cell free condition (Figure 1). We next used immunofluorescence staining to verify whether the assemblies formed by co-assembly of **Npx-1P** and **Npx-1** sequestrated the enzymes. Being incubated Saos-2 cells with **Npx-1P** (12.5 μM) after 0.5 h (Figure S15), both COX-2 and PTP1B form puncta and the green fluorescence from COX-2 start to overlap to red fluorescence from PTP1B at some regions. After 1 h incubation, more yellow fluorescence appears at the site of ER, indicating increased level of co-localization of the two enzymes (Figure 3B and C). Orthogonal Z-stack scanning (Figure 3D) also indicates the intracellular association of PTP1B and COX-2 upon incubation the cells with **Npx-1P**. We also examined the enzyme sequestration in HS-5 cells (as a control of Saos-2 cells since HS-5 express low level of ALPL[35]) and found that the addition of **Npx-1P** hardly induced the sequestration or co-localization of COX-2 and PTP1B in the cells (Figure S16). Together with our previous report[29] that EISA precursors hardly form assemblies in HS-5 cells, this result indicates cell selective formation of molecular condensates for enzyme sequestration by EISA.

To evaluate the specificity of intracellular enzyme sequestration by the assemblies formed by EISA, we used immunofluorescence staining to examine the interactions of COX-1, an isozyme of COX-2. As shown in Figure 4, COX-1 hardly forms puncta inside Saos-2 cells, indicating that the supramolecular assemblies of **Npx-1P** and **Npx-1** scarcely interact with COX-1 in Saos-2 cells. This results is likely due to the enhanced selectivity of **Npx-1P** towards COX-2,[27] suggesting that the strong interaction between the naproxen-peptide conjugates and COX-2 is critical for the sequestration of COX-2. To further verify the molecular basis of **Npx-1P** for the sequestration of COX-2 and PTP1B, we designed two control molecules (**Nap-1P**, **Npx-2P**) by mutating fragments in **Npx-1P** (Scheme S1). Replacing the naproxen with naphthalene in **Npx-1P** yields **Nap-1P**, which hardly induces the puncta formation of COX-2 or PTP1B, further confirming the importance of the COX-2 binding moiety (i.e., naproxen). Having a D-phosphoserine to replace the D-phosphotyrosine (in **Npx-1P**), **Npx-2P** fails to cause the association of PTP1B or COX-2, agreeing with that phosphoserine significantly diminishes PTP1B-substrate interaction[36,37] and self-assembling ability. These results, collectively, confirm the essential role of phosphotyrosine and naproxen for the sequestration of PTP1B and COX-2 by the assemblies of **Npx-1P** and **Npx-1**.

In conclusion, this work illustrated a novel strategy to sequestrate intracellular enzymes selectively via instructed-assembly. Incorporating with specific protein interaction motifs, the precursors, via EISA process, form supramolecular assemblies that display the protein-binding motifs on the surface of the molecular assemblies due to the dynamic and adaptive properties of the peptide assemblies, thus interacting with multiple proteins in a manner to

concentrate specific proteins (e.g., PTP1B and COX-2 in this work). This process is similar to formation of higher-order assemblies of proteins[38] or protein phase transition,[39] a ubiquitous phenomenon in biology for cell signaling. Moreover, employing synthetic small molecules to generate intracellular molecular assemblies (or condensates) represents a general way to create a multifunctional signal hub for modulating diverse protein-protein interactions,[40] especially for controlling protein-protein interaction involving tertiary epitopes that are much more dynamic.[41] Further exploration along this direction may lead to remarkable therapeutic benefits, as shown by the drugs that control protein-protein interactions.[42,43]

Supplementary Material

Refer to Web version on PubMed Central for supplementary material.

ACKNOWLEDGMENT

This work is partially supported by NIH (R01CA142746) and NSF (DMR-1420382). Z.F. is supported by NIH (F99CA234746).

REFERENCES

(1). Gall JG; Bellini M; Wu Z; Murphy C Assembly of the nuclear transcription and processing machinery: Cajal bodies (coiled bodies) and transcriptosomes. Mol. Biol. Cell 1999, 10, 4385–4402. [PubMed: 10588665]

(2). Liu JL; Gall JG U bodies are cytoplasmic structures that contain uridine-rich small nuclear ribonucleoproteins and associate with P bodies. Proc. Natl. Acad. Sci. U. S. A 2007, 104, 11655–11659. [PubMed: 17595295]

(3). Boisvert FM; van Koningsbruggen S; Navascues J; Lamond AI The multifunctional nucleolus. Nat. Rev. Mol. Cell Biol 2007, 8, 574–585. [PubMed: 17519961]

(4). Shin Y; Brangwynne CP Liquid phase condensation in cell physiology and disease. Science 2017, 357, eaaf4382. [PubMed: 28935776]

(5). Du M; Chen ZJ DNA-induced liquid phase condensation of cGAS activates innate immune signaling. Science 2018, 361, 704–709. [PubMed: 29976794]

(6). Brangwynne CP; Eckmann CR; Courson DS; Rybarska A; Hoege C; Gharakhani J; Julicher F; Hyman AA Germline P Granules Are Liquid Droplets That Localize by Controlled Dissolution/Condensation. Science 2009, 324, 1729–1732. [PubMed: 19460965]

(7). Li P; Banjade S; Cheng H-C; Kim S; Chen B; Guo L; Llaguno M; Hollingsworth JV; King DS; Banani SF; Russo PS; Jiang Q-X; Nixon BT; Rosen MK Phase transitions in the assembly of multivalent signalling proteins. Nature 2012, 483, 336–340. [PubMed: 22398450]

(8). Yang Z; Liang G; Xu B Enzymatic Hydrogelation of Small Molecules. Acc. Chem. Res 2008, 41, 315–326. [PubMed: 18205323]

(9). Zhou J; Xu B Enzyme-instructed self-assembly: a multistep process for potential cancer therapy. Bioconjugate Chem. 2015, 26, 987–999.

(10). He HJ; Xu B Instructed-Assembly (iA): A Molecular Process for Controlling Cell Fate. Bull. Chem. Soc. Jpn 2018, 91, 900–906. [PubMed: 30559507]

(11). Lock LL; Reyes CD; Zhang P; Cui H Tuning Cellular Uptake of Molecular Probes by Rational Design of Their Assembly into Supramolecular Nanoprobes. J. Am. Chem. Soc 2016, 138, 3533–3540. [PubMed: 26890853]

(12). Shamay Y; Shah J; Isik M; Mizrachi A; Leibold J; Tschaharganeh DF; Roxbury D; Budhathoki-Uprety J; Nawaly K; Sugarman JL; Baut E; Neiman MR; Dacek M; Ganesh KS; Johnson DC; Sridharan R; Chu KL; Rajasekhar VK; Lowe SW; Chodera JD; Heller DA Quantitative self-

assembly prediction yields targeted nanomedicines. Nat. Mater 2018, 17, 361–368. [PubMed: 29403054]

(13). Sato K; Ji W; Palmer LC; Weber B; Barz M; Stupp SI Programmable Assembly of Peptide Amphiphile via Noncovalent-to-Covalent Bond Conversion. J. Am. Chem. Soc 2017, 139, 8995–9000. [PubMed: 28639790]

(14). Ng KK; Takada M; Harmatys K; Chen J; Zheng G Chlorosome-Inspired Synthesis of Templated Metallochlorin-Lipid Nanoassemblies for Biomedical Applications. ACS Nano 2016, 10, 4092–4101. [PubMed: 27015124]

(15). Wang H; Feng Z; Wang Y; Zhou R; Yang Z; Xu B Integrating Enzymatic Self-Assembly and Mitochondria Targeting for Selectively Killing Cancer Cells without Acquired Drug Resistance. J. Am. Chem. Soc 2016, 138, 16046–16055. [PubMed: 27960313]

(16). Wang H; Feng Z; Wu D; Fritzsching KJ; Rigney M; Zhou J; Jiang Y; Schmidt-Rohr K; Xu B Enzyme-Regulated Supramolecular Assemblies of Cholesterol Conjugates against Drug-Resistant Ovarian Cancer Cells. J. Am. Chem. Soc 2016, 138, 10758–10761. [PubMed: 27529637]

(17). Feng Z; Wang H; Zhou R; Li J; Xu B Enzyme-Instructed Assembly and Disassembly Processes for Targeting Downregulation in Cancer Cells. J. Am. Chem. Soc 2017, 139, 3950–3953. [PubMed: 28257192]

(18). Pires RA; Abul-Haija YM; Costa DS; Novoa-Carballal R; Reis RL; Ulijn RV; Pashkuleva I Controlling cancer cell fate using localized biocatalytic self-assembly of an aromatic carbohydrate amphiphile. J. Am. Chem. Soc 2015, 137, 576–579. [PubMed: 25539667]

(19). Tanaka A; Fukuoka Y; Morimoto Y; Honjo T; Koda D; Goto M; Maruyama T Cancer cell death induced by the intracellular self-assembly of an enzyme-responsive supramolecular gelator. J. Am. Chem. Soc 2015, 137, 770–775. [PubMed: 25521540]

(20). Du X; Zhou J; Wang H; Shi J; Kuang Y; Zeng W; Yang Z; Xu B In situ generated D-peptidic nanofibrils as multifaceted apoptotic inducers to target cancer cells. Cell Death Dis. 2017, 8, e2614. [PubMed: 28206986]

(21). Liang C; Zheng D; Shi F; Xu T; Yang C; Liu J; Wang L; Yang Z Enzyme-assisted peptide folding, assembly and anti-cancer properties. Nanoscale 2017, 9, 11987–11993. [PubMed: 28792044]

(22). Wang H; Wei J; Yang C; Zhao H; Li D; Yin Z; Yang Z The inhibition of tumor growth and metastasis by self-assembled nanofibers of taxol. Biomaterials 2012, 33, 5848–5853. [PubMed: 22607913]

(23). Yuan Y; Wang L; Du W; Ding Z; Zhang J; Han T; An L; Zhang H; Liang G Intracellular Self-Assembly of Taxol Nanoparticles for Overcoming Multidrug Resistance. Angew. Chem., Int. Ed 2015, 54, 9700–9704.

(24). Ye DJ; Shuhendler AJ; Cui LN; Tong L; Tee SS; Tikhomirov G; Felsher DW; Rao JH Bioorthogonal cyclization-mediated in situ self-assembly of small-molecule probes for imaging caspase activity in vivo. Nat. Chem 2014, 6, 519–526. [PubMed: 24848238]

(25). Yuan Y; Sun HB; Ge SC; Wang MJ; Zhao HX; Wang L; An LN; Zhang J; Zhang HF; Hu B; Wang JF; Liang GL Controlled Intracellular Self-Assembly and Disassembly of F-19 Nanoparticles for MR Imaging of Caspase 3/7 in Zebrafish. ACS Nano 2015, 9, 761–768. [PubMed: 25544315]

(26). Zhan J; Cai YB; He SS; Wang L; Yang ZM Tandem Molecular Self-Assembly in Liver Cancer Cells. Angew. Chem., Int. Ed 2018, 57, 1813–1816.

(27). Li JY; Kuang Y; Gao Y; Du XW; Shi JF; Xu B D-Amino Acids Boost the Selectivity and Confer Supramolecular Hydrogels of a Nonsteroidal Anti-Inflammatory Drug (NSAID). J. Am. Chem. Soc 2013, 135, 542–545. [PubMed: 23136972]

(28). Gao Y; Shi JF; Yuan D; Xu B Imaging enzyme-triggered self-assembly of small molecules inside live cells. Nat. Commun 2012, 3.

(29). Feng Z; Wang H; Wang S; Zhang Q; Zhang X; Rodal AA; Xu B Enzymatic Assemblies Disrupt the Membrane and Target Endoplasmic Reticulum for Selective Cancer Cell Death. J. Am. Chem. Soc 2018, 140, 9566–9573. [PubMed: 29995402]

(30). Fogh J Human tumor cells in vitro; Plenum Press: New York, 1975.

(31). Whitesides GM Complex Organic Synthesis: Structure, Properties, and/or Function? Isr. J. Chem 2018, 58, 142–150.

(32). Merrifield RB SOLID PHASE PEPTIDE SYNTHESIS .1. SYNTHESIS OF A TETRAPEPTIDE. J. Am. Chem. Soc 1963, 85, 2149.

(33). Hirst AR; Roy S; Arora M; Das AK; Hodson N; Murray P; Marshall S; Javid N; Sefcik J; Boekhoven J; van Esch JH; Santabarbara S; Hunt NT; Ulijn RV Biocatalytic induction of supramolecular order. Nat. Chem 2010, 2, 1089–1094. [PubMed: 21107375]

(34). Ardoña HAM; Draper ER; Citossi F; Wallace M; Serpell LC; Adams DJ; Tovar JD Kinetically Controlled Coassembly of Multichromophoric Peptide Hydrogelators and the Impacts on Energy Transport. J. Am. Chem. Soc 2017, 139, 8685–8692. [PubMed: 28578581]

(35). Zhou J; Du XW; Berciu C; He HJ; Shi JF; Nicastro D; Xu B Enzyme-Instructed Self-Assembly for Spatiotemporal Profiling of the Activities of Alkaline Phosphatases on Live Cells. Chem 2016, 1, 246–263. [PubMed: 28393126]

(36). Sarmiento M; Zhao Y; Gordon SJ; Zhang ZY Molecular basis for substrate specificity of protein-tyrosine phosphatase 1B. J. Biol. Chem 1998, 273, 26368–26374. [PubMed: 9756867]

(37). Yudushkin IA; Schleifenbaum A; Kinkhabwala A; Neel BG; Schultz C; Bastiaens PIH Live-cell Imaging of enzyme-substrate interaction reveals spatial regulation of PTP1B. Science 2007, 315, 115–119. [PubMed: 17204654]

(38). Wu H; Fuxreiter M The Structure and Dynamics of Higher-Order Assemblies: Amyloids, Signalosomes, and Granules. Cell 2016, 165, 1055–1066. [PubMed: 27203110]

(39). Boeynaems S; Alberti S; Fawzi NL; Mittag T; Polymenidou M; Rousseau F; Schymkowitz J; Shorter J; Wolozin B; Van den Bosch L; Tompa P; Fuxreiter M Protein Phase Separation: A New Phase in Cell Biology. Trends Cell Biol 2018, 28, 420–435. [PubMed: 29602697]

(40). van Dun S; Ottmann C; Milroy LG; Brunsveld L Supramolecular Chemistry Targeting Proteins. J. Am. Chem. Soc 2017, 139, 13960–13968. [PubMed: 28926241]

(41). Arkin MR; Tang Y; Wells JA Small-Molecule Inhibitors of Protein-Protein Interactions: Progressing toward the Reality. Chem. Biol (Oxford, U. K.) 2014, 21, 1102–1114. [PubMed: 25237857]

(42). Souers AJ; Leverson JD; Boghaert ER; Ackler SL; Catron ND; Chen J; Dayton BD; Ding H; Enschede SH; Fairbrother WJ; Huang DCS; Hymowitz SG; Jin S; Khaw SL; Kovar PJ; Lam LT; Lee J; Maecker HL; Marsh KC; Mason KD; Mitten MJ; Nimmer PM; Oleksijew A; Park CH; Park CM; Phillips DC; Roberts AW; Sampath D; Seymour JF; Smith ML; Sullivan GM; Tahir SK; Tse C; Wendt MD; Xiao Y; Xue JC; Zhang HC; Humerickhouse RA; Rosenberg SH; Elmore SW ABT-199, a potent and selective BCL-2 inhibitor, achieves antitumor activity while sparing platelets. Nat. Med 2013, 19, 202–208. [PubMed: 23291630]

(43). Schiff PB; Horwitz SB Taxol stabilizes microtubules in mouse fibroblast cells. Proc. Natl. Acad. Sci. U. S. A 1980, 77, 1561–1565. [PubMed: 6103535]

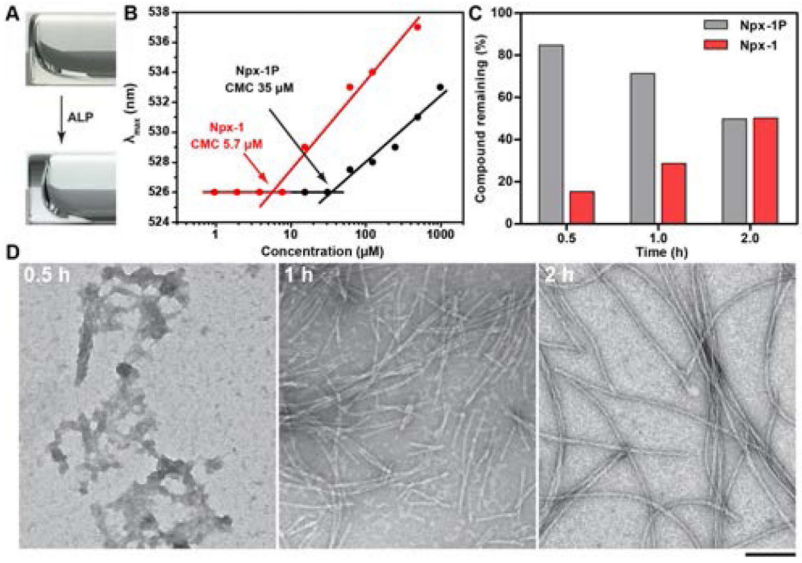

Figure 1.

(A) Sol-gel transition of **Npx-1P** (400 μM) upon adding ALP (1 U/mL). (B) CMCs of **Npx-1P** and **Npx-1**. (C) Dephosphorylation of **Npx-1P** (12.5 μM) after incubating with 0.1 U/mL ALP at different time. (D) TEM images of nanostructures formed before and after adding ALP (0.1 U/mL) to the solution of **Npx-1P** (12.5 μM)(scale bar = 100 nm). All the solutions were prepared in pH 7.4 PBS buffer.

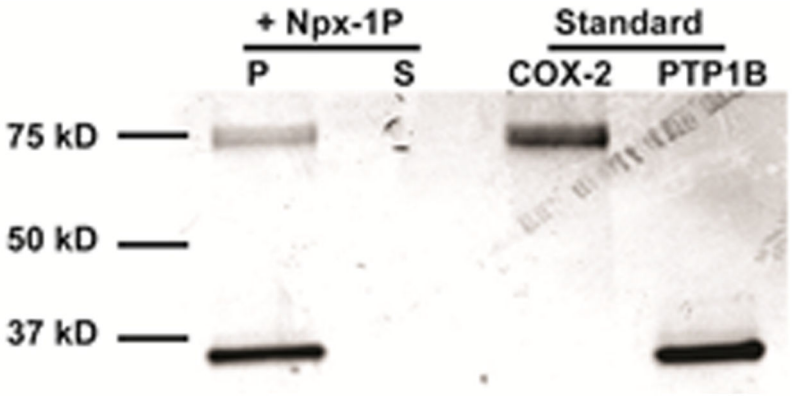

Figure 2.

Pull down of COX-2 and PTP1B with enzymatic assemblies formed by **Npx-1P** in PBS. The image shows Coomassie staining of pellet (P) and supernatant (S) fractions.

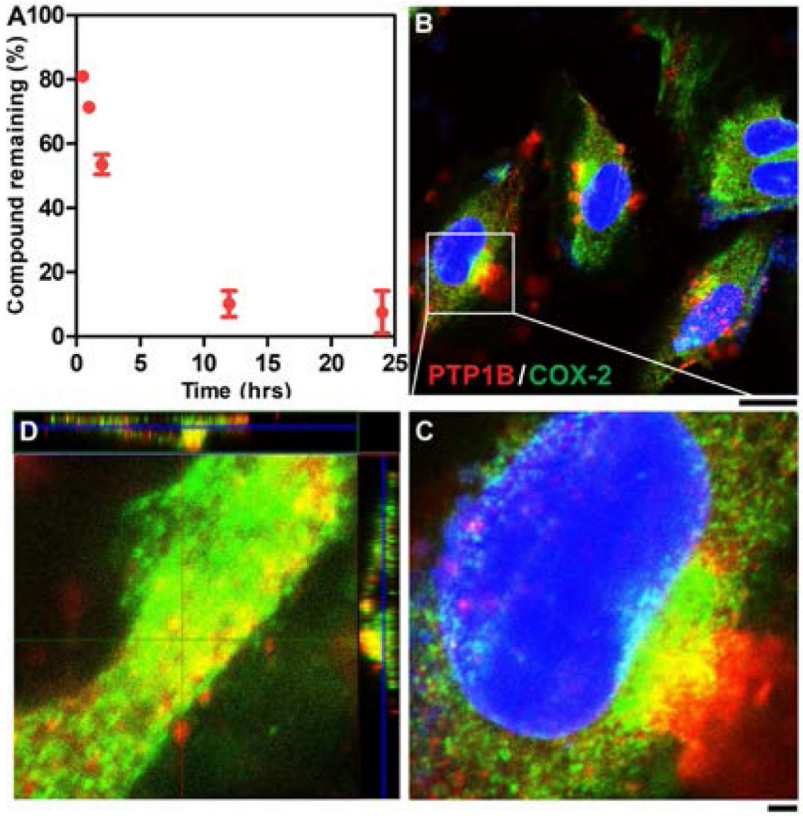

Figure 3.

(A) Dephosphorylation of **Npx-1P** (12.5 μM) after incubating with Saos-2 cells at different time. (B) CLSM images of Saos-2 cells treated with **Npx-1P** (12.5 μM) for 1 h and then stained with antibodies of PTP1B (red) and COX-2 (green). (C) The enlarged region of co-localization in (B) (scale bar = 2 μm). (D) Orthogonal Z-stack of co-localization of PTP1B and COX2.

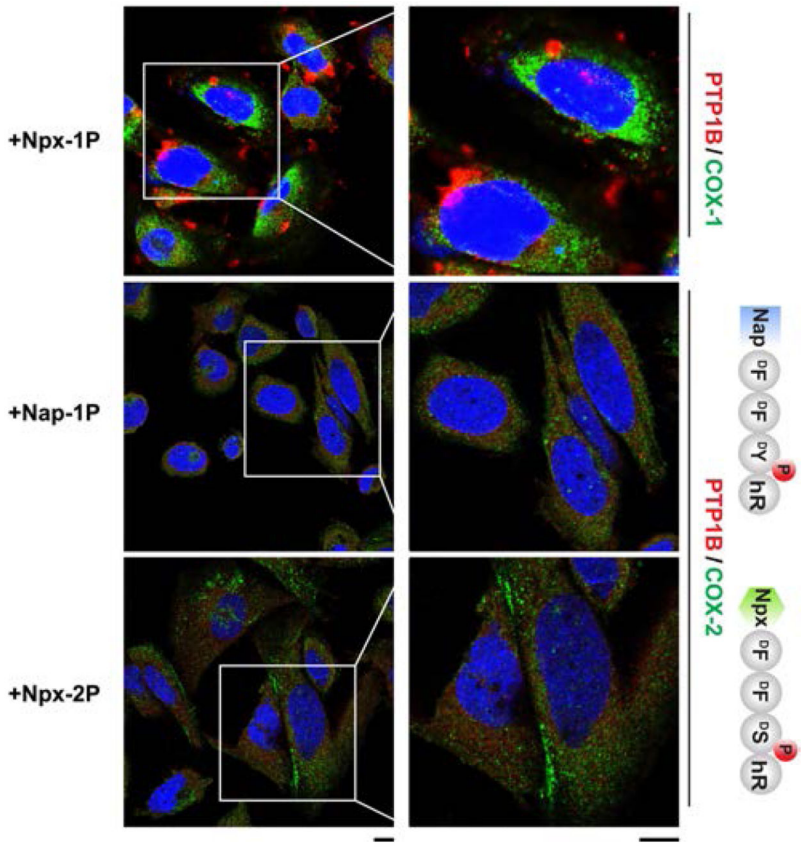

Figure 4.

CLSM images of Saos-2 cells stained with antibodies of PTP1B (red) and COX-1/COX-2 (green) after treating with **Npx-1P**, **Nap-1P** and **Npx-2P** for 1 h (scale bar = 10 μm).

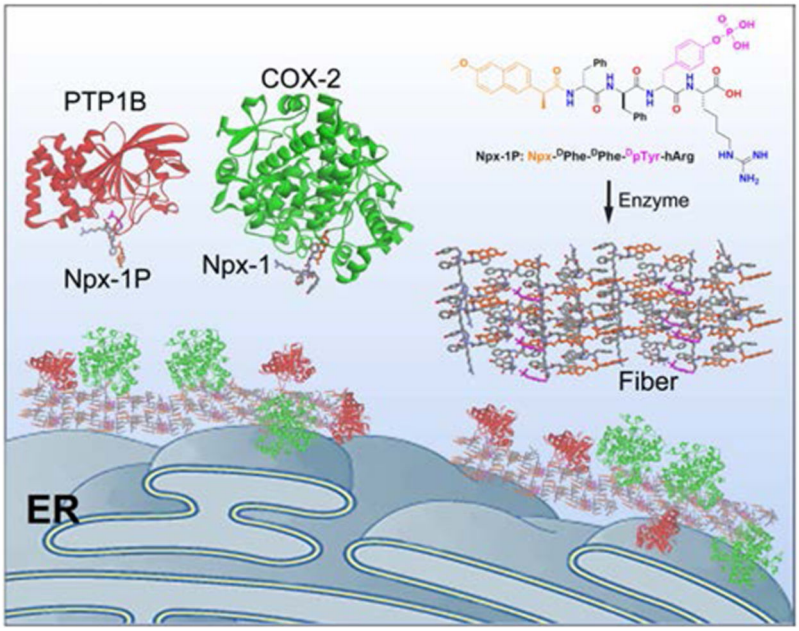

Scheme 1.
Illustration of instructed-assembly for intracellular sequestration of PTP1B and COX-2.